2nd IFAC Workshop on Automatic Control in Offshore Oil and Gas Production,
May 27-29, 2015, Florianópolis, Brazil

Linear Serial Elastic Hydraulic Actuator: Digital Prototyping and Force Control

Arnaldo Gomes Leal Junior*, Rafhael Milanezi de Andrade**
Antônio Bento Filho***

Department of Mechanical Engineering, Universidade Federal do Espirito Santo, 29075-910 ES, Brazil
**(e-mail: arnaldo_lealjunior@hotmail.com).*
*** (e-mail: rafhael.andrade@ufes.com)*
**** (e-mail: antonio.bento@ufes.br)*

Abstract: In aggressive environments for humans, such as those present in the offshore industry, the main alternative is to replace human labor by remotely controlled robots, and some cases completely autonomous robots. The environment affects directly on robots tasks. When a robot works in a structured environment, its automation is easier since the environment can be modeled by dynamics equations. However if the environment is non-structured this modeling is quite difficult and presents a high computational effort. To overcome this difficult, over the years series elastic actuator (SEA) has been applied in non-structured environments. Actuators of the mechanical systems are always rigidly connected to the load to be moved. This can be observed in the hydraulic systems of agricultural, highway construction and mining equipment and in elevation and cargo transportation, among others. Unlike rigid actuators, a SEA contains an elastic element in series with the mechanical energy source. Such an elastic element gives SEA's several unique properties compared to rigid actuators, including tolerance to impact loads, low mechanical output impedance, passive mechanical energy storage, and increased peak power output. However it is not trivial to select the correct spring for the system. The spring has to be able to support the loads, but the spring cannot be too stiff, otherwise system impedance will be high. Iterative methods are needed to select the spring, which fits in impedance and bandwidth parameters. The resonance frequency is another issue for SEAs. This paper describes an entire digital prototyping of a linear serial elastic hydraulic actuator. It is done a digital prototyping of a tubular actuator design, which encapsulates the mechanical and electrical components and sensors. The digital prototype dimensions, mass and inertia properties are used to build the dynamic model for simulations and implementation of a controller. Moreover the methodology adopted results in a good response actuator with a compact and high force design.

Keywords: SEA, hydraulic actuators, servo hydraulics, PID control, force control.

1. INTRODUCTION

Trends in the oil and gas industry to improve safety and efficiency and reduce environmental impact suggest the use of industrial robotics. New developments in regions difficult or dangerous for humans to work in could be enabled with maintenance, inspection and repairs carried out by remotely controlled industrial robots. This new application area highlights some difficulties with today's robots, as they do not adapt well to dynamic environments. Therefore, new decision models, methods of control, actuators need to be developed.

Series elastic actuator (SEA) has been successfully used in a number of applications for almost 20 years (Pratt and Williamson, 1995). As widely reported by a number of researchers (see (Pratt and Williamson, 1995), (Arumugom et al. 2009), (Paluska and Herr, 2006) and (Paine et al, 2013)) series elastic actuators provide many benefits in force control of robots. Unlike rigid actuators, SEA's contain an elastic element in series with the mechanical energy source. Such as elastic element gives SEA's several unique properties compared to rigid actuators including low mechanical output impedance, tolerance to impact loads, increased peak power output, and passive mechanical energy storage. These properties are well aligned with requirements on legged actuation systems; as a result, SEA's have been widely adopted in the fields of legged robotics and human orthotics (Parietti et al., 2011)).

The SEA's components can be chosen and configured in many different ways, producing designs with various trade-offs which affect the power output, volumetric size, weight, efficiency, back drivability, impact resistance, passive energy storage, backlash, and torque ripple of a SEA. (Kong et al, 2009), and (Ragonesi et al., 2011) propose rotary designs based primarily on commercially available off-the-shelf components. (Lagoda et al., 2010) and (Diftler et al., 2011) design a compact rotary SEA using a harmonic drive and a high-stiffness planar spring.(Hutter et al. 2011) use linear springs coupled to rotary shafts between the motor and the chassis ground to achieve compact actuator packaging with low spring stiffness. In (Taylor, 2011), the authors placed the spring within the reduction phase. This arrangement reduces the torque requirement on the spring compared to designs with the spring at the actuator output. (Pratt and Pratt, 1998) propose a prismatic designs which use ball screws as the primary reduction mechanism followed by a cable drive to remotely drive a revolute joint. Ball screws are highly efficient, even for large speed reductions (85–90%), are back

drivable, are tolerant to impact loads, and do not introduce torque ripple. (Paine et al., 2013) is a good review of some recent progress in series elastic actuators. In this paper it is presented a different design of a SEA. In order to avoid accidents risks and components contamination, the internal components were encapsulated in a unique hollow tubular structure. That allows substitute the heavy structure of solid steel tubes of the reference model (Pratt et al., 2002), permitting the applications in wearable robots, exoskeletons and prostheses.

Different control architectures have been proposed for controlling series elastic actuators. The variation of controller design is related to the different physical characteristics of the hardware. For example, force can be observed either by measuring spring deflection and applying Hooke's law in (Kong et al., 2010), or by measuring change in resistance, as is accomplished using strain gauges, as shown in (Pratt and Williamson, 1995). If friction and backlash are too large, a pure high-gain PID approach can suffer from stability issues. In order to avoid this issue, (Pratt et al., 2004) suggest using position feedback as the innermost control structure for force control. This idea is adopted in others researches see (Lagoda et al., 2010), treating force control as a position or velocity-tracking problem.

In general, the SEAs can be actuated by electrical source, pneumatic cylinder, hydraulic cylinder. The hydraulic SEA is similar to a SEA with electrical source replacing the electrical source, which is a motor with a recirculating ball screw by a hydraulic cylinder. According (Prat et al., 2002) a hydraulic SEA has high output force with force and position controllability.

In this paper the digital prototyping of a hydraulic SEA is developed. The methodology showed in (Robinson and Pratt, 2000) is used specially to choose the spring stiffness. The dynamic model has to contemplate the hydraulic cylinder internal leakage (Qian et al., 2014) and a PID controller has to be designed by pole placement and phase margin (Tang et al., 2010).

The hydraulic SEA developed here is a contribution for robot's desing for non-structured enviorement, in special for oil and gas aplication since this industry applies robots on drilling platforms which uses the Remotely Operated Vehicle (ROV). The ROVs have two actuators on each ROV manipulator which can be replaced by two hydraulic SEAs for more force with less weight. The impact tolerance provides one of the major advantages of a hydraulic SEA increasing actuator durability and smooth contact which makes the actuator suitable to operating valve. The serial elastic element provides that impact tolerance and it makes the possibility of contact inspection on pipe by spring deflection analysis for example.

2. METHODOLOGY

A basic model of a serial elastic hydraulic actuator has the serial element i.e. a rod with the spring's arrangement and a hydraulic circuit which contains the hydraulic cylinder and the servo valve.

The actuator may be understood as a combination of two parts. The first one is the serial elastic element presented in Figure 1. The other one is the hydraulic circuit which has some alternatives of construction as well.

With the components of the actuator defined, the next step is to select the correct component based on the application. This decision is made defining a condition for this system. In this case the condition was the actuator with an output force up to 5000N.

To achieve the output force required, the springs were selected based on consolidate knowledge presented by mechanical engineering design bibliography. Moreover, the rod had to be able to support the load without buckling. Therefore, the knowledge presented by the solid mechanics bibliography is able to help with the design of the desirable rod by considering the systems behavior with all loads.

A special attention must be given to the actuator's springs because they affect system's impedance and bandwidth. After setting these two parameters, iteration could be necessary to evaluate the desirable spring constant.

Knowing the rod and the spring, it is possible to use the force caused by the spring as the force output of the hydraulic cylinder. This force and the maximum speed of 0.5 m/s (as defined by Robinson and Pratt (2000) led to the selection of the correct cylinder by a commercial catalogue, otherwise would be possible to manufacture a custom cylinder.

After design the parts it is assembled in a digital prototyping environment. The parts are drawn using the Siemens Solid Edge software which allows obtaining inertial properties of the assembly.

The actuator's dynamic model was developed from well-known mass-spring-damping system and the actuator's hydraulic part, which is the most challenging, was developed by all hydraulic system components analysis with linearization and simplification as defined in (Qian et al.,2014).

The PID control was obtained by a method based on pole placement and phase margin as defined in (Tang et al., 2010). After the tuning, the time response and the bode diagram of the system were analysed in order to describe system's characteristics of force control.

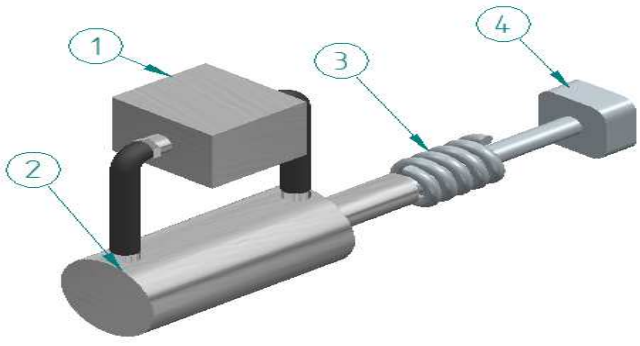

Fig.1. Single rod hydraulic serial elastic actuator schematics: (1) servo valve; (2) hydraulic cylinder; (3) spring; (4) load.

3. DIGITAL PROTOTYPING DESIGN

Over the years, digital prototyping has been successfully applied in engineering and manufacturing allowing virtually explore a complete product before it's built ((Thurfjell et al., 2002), (Soyguder and Alli, 2007), and (Wang, 2011)). As reported by Johansson et al. (2004), the digital prototyping has been important to development of industrial robots, reducing the time of robot-programming phase. The robot task can be simulated in a virtual model of the work cell when still only a digital prototype of the work piece exists and the risk of technical failure for a transition can be reduced. In this way, before manufacture of the proposed serial elastic actuator, is presented in this paper its digital prototyping.

3.1 Model

The design was done by the methodology mentioned on the previous section. Following these steps, the actuator had the maximum output force with the most compact design. Also all the internal components had been enclosed to avoid accidents, components contamination and make the actuator suitable to human interaction.

Figure 2 shows the prototype of the actuator. There is a hydraulic cylinder (1) that moves forward and dislocates the movable rod (2) fixed in it with a screwed connection. The model has two guides (6) and (8) fixed on the base tube and one guide (7) fixed on movable rod (2). There are two springs (4) and (5) fixed between the guides. A connection guide (10) is used to connect the hydraulic cylinder rod (1) to the base tube (3). The load terminal (9) is also connected directly on the base tube (3). The encapsulation tube (12) is the last part of the assembly. It is connected on the hydraulic cylinder (1) and base tube (3). A guide bolt (11) was applied to make the connection between the base tube (3) and the encapsulation tube (12), but without interfere on the base tube's (3) linear movement.

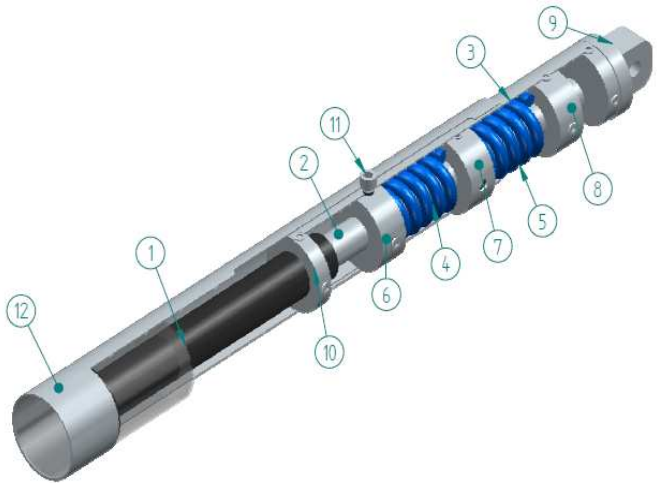

Fig.2. Actuator's components: (1) hydraulic cylinder; (2) movable rod; (3) base tube; (4) and (5) springs; (6), (7) and (8) guides; (9) load terminal; (10) connection guide; (11) guide bolt; (12) encapsulation tube.

There are four guides (6), (7), (8), and (10) in this actuator model. The application of the four guides is to give to the system the necessary stability. Without the guides the movable rod (2) would oscillate creating additional forces on the springs instead of only an axial force. Moreover, the load terminal is connected with the base tube only.

The springs are responsible to the hydraulic SEA stiffness reduction. However this component has to be carefully assembled since it will stretch and compress depending on the movement of the actuator and the load attached to it. Choosing the spring is always challenging, because it has to be a balance between a large bandwidth requiring a high stiffness and impedance need a low spring constant. Therefore, after choose all system characteristics and components, must be defined a minimum acceptable point for the large force bandwidth and a minimum tolerance impedance level. After set these two bounds, iteration is required to estimate the spring constant.

The movement of the actuator can be analysed in three different cases:

Case 1: Movement without the load

This is the simplest case, because it is a free movement. The hydraulic cylinder moves forward or backward and the movable rod and all the others components attached to it such as base tube, guides and load terminal follow the move of the hydraulic cylinder. In this case, there is only a little deflection in the spring by the inertia.

Case 2: Movement with load

When a load is attached in the load terminal, the movement of the actuator depends on the springs. For a forward movement, the spring (4) deflects. This deflection depends of the load mass. The actuator will move forward only when the spring reaches its maximum deflection for the load applied. This system characteristic can reduce the frequency range, which makes a limit of bandwidth of the system, which is the major drawback of a serial elastic actuator.

For the backward movement the same characteristics can be observed, but the spring (4) deflects instead of the spring (5).

Case 3: Contact of the load terminal with the load

When the actuator reaches an obstacle or the load during its free movement, the spring (5) deflects and the value of this deflection makes the actuator continues its forward movement or stop.

The prototype shows outstanding characteristics of output force and compactness. These characteristics are listed as follows:

- 200 mm length when retracted;
- 100 mm range;
- Maximum diameter of 26 mm;
- Maximum output force up to 4.9 kN;

- 100 bar of working pressure;
- Model structure material of carbon steel;
- Speed up to 0.5 m/s;
- Estimated weight without hydraulic fluid of 1.5 kg.

Comparing this hydraulic SEA parameters with the electric SEA parameters (Bento Filho et al., 2014) and (Bento Filho et al., 2013), serial elastic hydraulic actuator is more suitable for applications involving high force and compactness.

3.2 Sensors

Actuator's parameters are measured for modelling and control proposes. Important parameters were the deflection of the springs and the displacement of the movable rod, which happened due the movement of the hydraulic cylinder.

A linear potentiometer was chosen to evaluate the movable rod's displacement. The potentiometer did not have the resolution to evaluate the deflection of the springs which is about 8 mm, therefore a different sensor was chosen to evaluate this deflection.

The sensor chosen to evaluate springs deflection was an optical sensor used on a printer. This sensor has a scaled tape with black lines, with distance between the lines known, which does not allow light beam passage. The tape movement produces pulses, which are proportional to spring deflection.

The assembly of the sensors was shown on the Figure 3 above. The linear potentiometer (3) was connected directly on the hydraulic cylinder rod (2) and the hydraulic cylinder bore (1). The optical sensor has a circuit board (7) with a sensor (9). This circuit board was connected on the guide (6) by a bolt connection, which was not represented in the figure. The optical tape (8) was connected on the guides (4) and (5) by a bolt connection and positioned on the optical sensor (9).

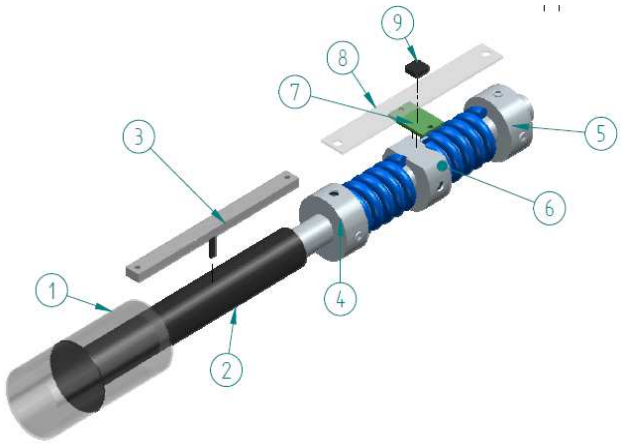

Fig.3. Sensors assembly: (1) hydraulic cylinder bore; (2) hydraulic cylinder rod ;(3) linear potentiometer; (4), (5) and (6) guides; (7) circuit board; (8) optical sensor tape; (9) optical sensor.

4. DYNAMIC MODEL

The system consists of a servo-hydraulic system with a serial elastic element. The overall system has two degree of freedom. One degree is the hydraulic cylinder displacement and the other is the serial elastic element displacement. This displacement and the spring deflection were used to define the output force of the system and to control it.

Figure 4 illustrates the mechanical model of this system discussed above.

The servo-hydraulic system was made by a hydraulic power supply, servo valve acting as a control element and the hydraulic cylinder, which is the actuating element.

Although most of the servo-hydraulic system is nonlinear, each component of this model has been linearized.

The servo valve's pilot stage is assumed to be first order, since high order dynamics in the valve are more than an order of magnitude above the frequency range of interest. Equation 1 represents the servo valve pilot stage equation as seen in (Qian et al.,2014).

$$\frac{Q_s(s)}{v_i(s)} = \frac{K_{vp}}{\tau s + 1} \times K_p \times K_C \times K_v \quad (1)$$

Where K_{vp} is the flow gain of the pilot-stage servo valve and τ pilot-stage's equivalent time constant, v_i valve control signal transmitted from the hydraulic system internal proportional controller, K_P represents inner loop proportional gain, K_C is the valve pressure gain which relates flow from the pilot stage with spool position. The coefficient K_v is the flow gain of the servo valve and Q_s is the supply flow.

$$\frac{F_A(s)}{Q_s(s)} = \frac{\frac{4}{\beta V s + C_l} \times A}{1 + \frac{4}{\beta V s + C_l} \times A^2 \times X_1(s) s} \quad (2)$$

This β is the fluid bulk modulus, V is the fluid volume and P_l load pressure, A is the area, X(s) is the displacement of the assembly.
The serial elastic element has to be modeled by Newton's second law. The properties of the movable rod and the springs are considered on the stiffness, damping and mass terms. The load characteristics are also considered in the actuator's dynamic model.

$$X_1(s)(ms^2 + Cs + K) = F(s) \quad (3)$$

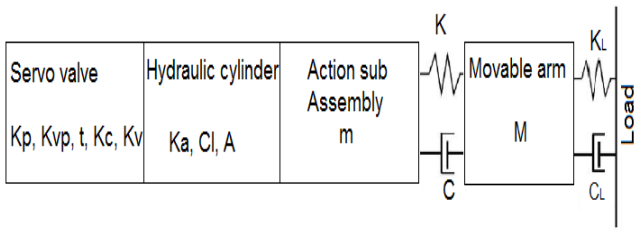

Fig. 4 Actuator's mechanical model.

X(s) is the assembly displacement, m is the sub assembly mass, C is the damping coefficient, K is the stiffness coefficient and F is the output force.

$$X_2(s)(Ms^2 + C_L s + K_L) = F(s) \quad (4)$$

M is the movable arm mass, C_L and K_L are the load interface viscous friction coefficient and load interface elastic constant respectively. $X_2(s)$ is the movable arm displacement.

The simplified closed loop transfer function block diagram for the dynamic model presented is the following on figure 5.

Each subsystem presented in the figure has a transfer function according the equation discussed on this topic. The actuator was modeled to have a natural velocity feedback. The leakage of the servo valve stages was neglected.

Several assumptions had been made in this model according (Qian et al.,2014):

- Fluid properties are constant;
- Servo valves are not saturated;
- Supply pressure is much greater than the load pressure;
- Friction force can be modeled as viscous damping;
- Main stage spool opening is proportional to pilot stage flow.

5. RESULTS AND DISCUSSION

Once described the actuator dynamic model, the parameters values had to be established. The parameters were obtained by the digital prototype and catalogue of some components i.e. servo valve and hydraulic actuator.

Spring constant is the most valuable parameter in the system. To define the spring constant were set the minimum impedance level and a maximum bandwidth with respect on the previous selected components of the hydraulic system. Iteration was made to choose the best value with upper and lower bounds.

After know all the actuator's parameters the PID controller could be designed. The controller was tuned by applying the pole placement and phase margin method (Tang et al., 2010).

Desired pair of poles is estimated by representing time domain specification e.g. percent overshoot, settling time. However in some cases the dominant poles lose its dominant position in the result of the closed loop system. To overcome this problem, a phase margin is employed to guarantee the closed loop system robustness.

Assuming a pair of poles as

$$p_{1,2} = -\alpha \pm j\beta \quad (5)$$

The process G(s) is given and the controller has its conventional configuration with all positive gains as follows.

$$C(s) = K_p + \frac{K_i}{s} + K_d s \quad (6)$$

Substituting one of the poles into the characteristic equation of the closed loop equation.

$$1 + G(p_1)C(p_1) = 0 \quad (7)$$

Table 1 shows the parameters value of the entire system.

Parameter	Value	Units
Area (A)	4.91E-04	(m^2)
Stiffness (K1)	7.5E+07	(N/m)
Damping (C1)	18.4	(Ns/m)
Mass (M)	1.5	(Kg)
Bulk modulus (B)	1.23E+09	(Pa)
Leakage Coefficient (Cl)	2E-06	(m^3s/kPa)
Fluid volume (Vt)	2.60E-05	m^3
Load stiffness (KL)	3.30E+09	(N/m)
Load damping (CL)	8.08	(Ns/m)
Inner loop gain (Kp)	8.40E+02	(s^-1)
Valve pressure gain (Kc)	4.00E+06	(m^3s/m)
Valve flow gain (Kv)	6.24E-05	(m^3s/m)
Servo valve time constant (t)	0.0015	(s)

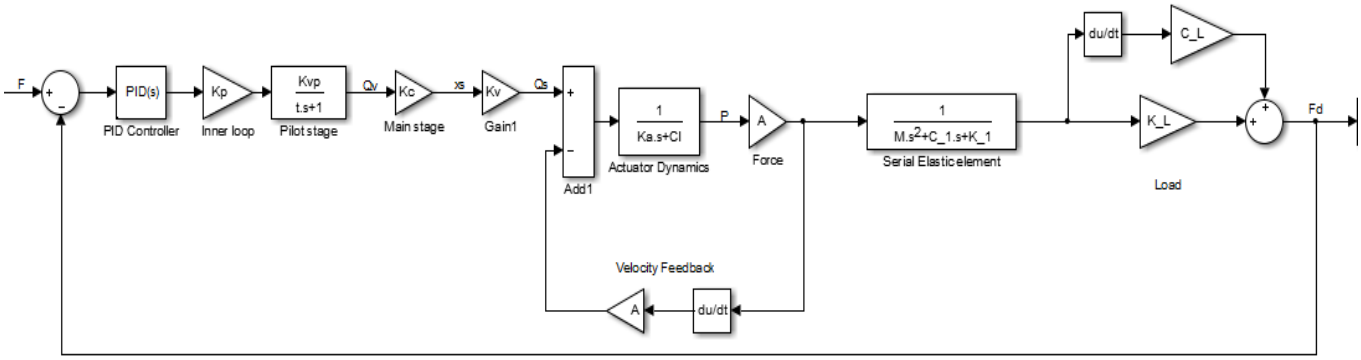

Fig.5. Closed loop transfer function block diagram

Moreover, the definition of phase margin gives:

$$G(j\omega_g)C(j\omega_g) = -e^{j\phi_m} \quad (8)$$

Substituting and splitting the complex equations into real ones gives two real functions of ω.

$$f_1(\omega) = \mathrm{Re}\left[\frac{-p_1}{G(p_1)}\right] + \frac{\alpha^2-\beta^2}{2\alpha\beta}\mathrm{Im}\left[\frac{-p_1}{G(p_1)}\right] + \frac{\alpha^2+\beta^2}{2\alpha}\mathrm{Re}\left[\frac{-e^{j\phi_m}}{G(j\omega)}\right] \quad (9)$$

$$f_2(\omega) = \frac{\omega^2}{2\alpha}\mathrm{Re}\left[\frac{-e^{j\phi_m}}{G(j\omega)}\right] - \frac{\omega^2}{2\alpha\beta}\mathrm{Im}\left[\frac{-p_1}{G(p_1)}\right] - \omega\,\mathrm{Im}\left[\frac{-e^{j\phi_m}}{G(j\omega)}\right] \quad (10)$$

The positive values of the intersection between $f_1(\omega)$ and $f_2(\omega)$ are the first approximation for integral gain (Ki). This first value was applied to evaluate the proportional and derivative gains. Proportional and derivative gains are obtained as follows.

$$K_p = \frac{2\alpha}{\alpha^2+\beta^2}\left(K_i - \mathrm{Re}\left[\frac{-p_1}{G(p_1)}\right] - \frac{\alpha^2-\beta^2}{2\alpha\beta}\mathrm{Im}\left[\frac{-p_1}{G(p_1)}\right]\right) \quad (11)$$

$$K_d = \frac{1}{\alpha^2+\beta^2}\left(K_i - \mathrm{Re}\left[\frac{-p_1}{G(p_1)}\right] - \frac{\alpha}{\beta}\mathrm{Im}\left[\frac{-p_1}{G(p_1)}\right]\right) \quad (12)$$

The final integral gain is the maximum value between the following equations.

$$K_{i,1} = \left(\mathrm{Re}\left[\frac{-p_1}{G(p_1)}\right] - \frac{\alpha}{\beta}\mathrm{Im}\left[\frac{-p_1}{G(p_1)}\right]\right) \quad (13)$$

$$K_{i,2} = \left(\mathrm{Re}\left[\frac{-p_1}{G(p_1)}\right] - \frac{\alpha^2-\beta^2}{2\alpha\beta}\mathrm{Im}\left[\frac{-p_1}{G(p_1)}\right]\right) \quad (14)$$

To achieve a robust control with large bandwidth it was set an overshoot about 10% and a settling time of 0.02 s. Phase margin was set 60°.

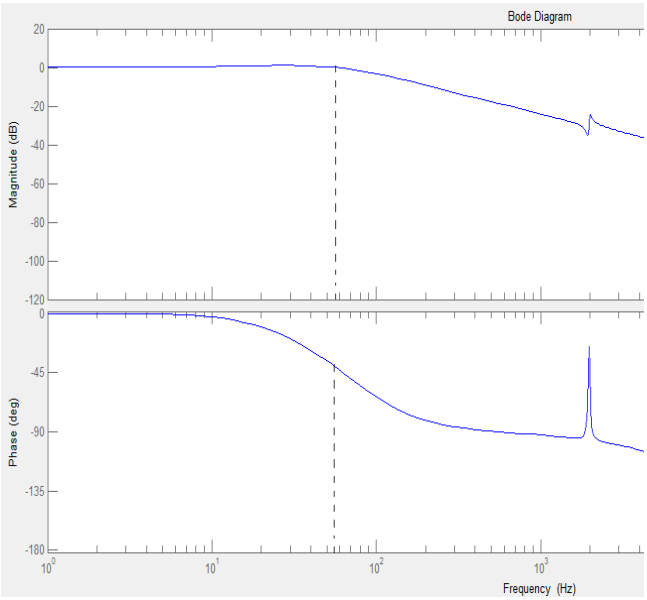

Fig.6. Bode diagram of the system

Table 2 shows the controller parameters.

Parameter	Value
Proportional gain (Kp)	54.9946
Integral gain (Ki)	4412.1219
Derivative gain (Kd)	0.0575

The bode diagram of the system (figure 6) shows an excellent frequency band of about 60 Hz which was greater than all references works presented (Bento Filho et al., 2014), (Paine et al., 2013), (Robinson and Pratt, 2000) and (Bento Filho et al., 2013). The phase angle for this frequency band was around 45°. The resonance frequency of the system was 1970 Hz which is far enough of system's operation frequency. This implies that the effects due to vibrations are efficiently filtered into the frequency band of the actuator.

To show the system's response, a hypothetical 1N desired force reference was applied. Figure 7 shows the system's response it could be seen the settling time around 0.02 seconds which was a very fast convergence to this system. The maximum overshoot was a little higher than 10% which was an acceptable value.

6. CONCLUSIONS

This paper presented a digital prototyping of a linear serial elastic hydraulic actuator for non-structural environments such as present in oil and gas industry. It was used a digital prototyping environment for design and assembly of actuators parts, generation of images of section views in perspective and exploded views, and all fabrication drawings of the parts of the actuator. The model obtained was very compact with a high output force which is desirable for all applications.

It also presented a dynamic model with a PID control which described the linear characteristics of the actuator. The system showed a good time and frequency responses.

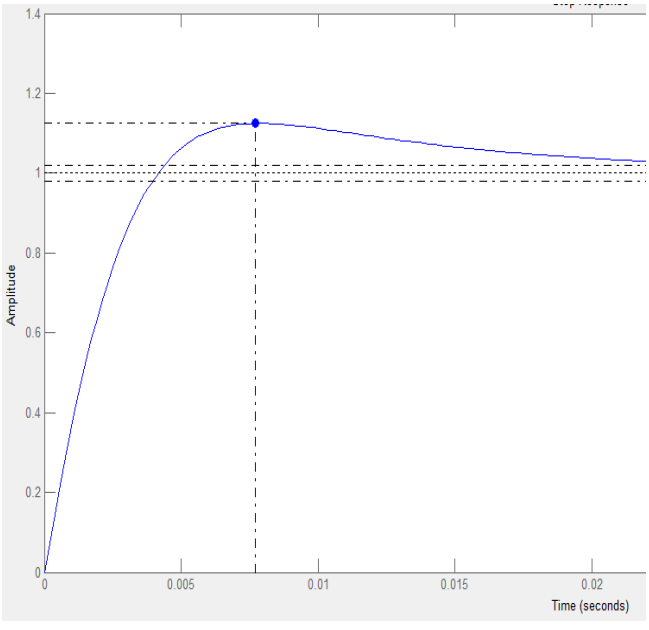

Fig.7. Time response of the system

The results obtained help the robots manipulators development for non-structured environments with another level of compactness and force capacity.

Future work develops another approach of the actuator's dynamic model. This new dynamic model considers the internal leakage on the servo valve, the saturation and more general friction force modelling. A better control technique is applied to improve force control of the nonlinear system. Another future work is an investigation of benefits and limitations of this actuator on a four legged dynamic robot.

REFERENCES

Arumugom, S., Muthuraman, S., and Ponselvan, V. (2009). "Modeling and application of series elastic actuators for force control multi legged robots," J. Comput., vol. 1, no. 1, pp. 26–33.

Bento Filho, A.; Mattos, M; Nossa, R.; Pretti, I., (2013). "Digital Prototyping of a Linear Electric Actuator with Serial Elastic Element" in Robot 2013: First Iberian Robotics Conference.

Bento Filho, A., Andrade, R, Mattos, M., (2014). "Digital prototyping of a series elastic actuator for exoskeletons" in CONEM 2014.

Diftler, M., Mehling, M., Abdallah, M., Radford, N., Bridgwater, L., Sanders, A., Askew, R., Linn, D., Yamokoski, J., Permenter, F., Hargrave, B., Piatt, R, Savely, R., and Ambrose, R. (2011). "Robonaut 2—The first humanoid robot in space," in Proc. IEEE Int. Conf. Robot. Autom., pp. 2178–2183.

Hutter, M., Remy, C., Hoepflinger, M., and Siegwart, R. (2011). "ScarlETH: Design and control of a planar running robot," in Proc. IEEE/RSJ Int. Conf. Intell. Robot. Syst., pp. 562–567.

Kong, K., Bae, J., and Tomizuka, M., (2009). "Control of rotary series elastic actuator for ideal force-mode actuation in human-robot interaction applications," in IEEE/ASME Trans. Mechatronics, vol. 14, no. 1, pp. 105–118.

Kong, K., Bae. J., Tomizuka, M., (2010). "A compact rotary series elastic actuator for knee joint assistive system," in Proc. IEEE Int. Conf. Robot. Autom., pp. 2940–2945.

Lagoda, C., Schouten, A., Stienen, A., Hekman, E., and van der Kooij, H. (2010). "Design of an electric series elastic actuated joint for robotic gait rehabilitation training," in Proc. IEEE 3rd RAS and EMBS Int. Conf. Biomed. Robot. Biomechatron. 2010, pp. 21–26.

Paine, N., Oh, S., and Sentis, L. (2013). "Design and Control Considerations for High-Performance Series Elastic Actuators" IEEE/ASME Trans. Mechatronics, vol. PP, Issue. 99, pp. 1–12.

Paluska, D. and Herr, H. (2006). "Series elasticity and actuator power output," in Proc. IEEE Int. Conf. Robot. Autom., pp. 1830–1833.

Parietti, F., Baud-Bovy, G., Gatti, E., Riener, R., Guzzella, L., and Vallery, H. (2011). "Series viscoelastic actuators can match human force perception," IEEE/ASME Trans. Mechatronics, vol. 16, no. 5, pp. 853–860.

Pratt, G. and Williamson, M. (1995). "Series elastic actuators," in Proc. IEEE/RSJ Int. Conf. Intell. Robot. Syst. Human Robot Interact. Cooper. Robot., vol. 1, pp. 399–406.

Pratt, G., Willisson, P., Bolton, C., and Hofman, A. (2004). "Late motor processing in low-impedance robots: Impedance control of series-elastic actuators," in Proc. Amer. Control Conf., vol. 4, pp. 3245–3251.

Pratt J., and Pratt, G. (1998). "Intuitive control of a planar bipedal walking robot," in Proc. IEEE Int. Conf. Robot. Autom., vol. 3, pp. 2014–2021.

Pratt, J., Krupp B., and Morse C. (2002). "Series elastic actuators for high fidelity force control", Industrial Robot: An International Journal, vol. 29, no 3, p. 234-241.

Qian, Y., Ou G., Maghareh, A., Dyke, S.J. (2014). "Parametric identification of a servo-hydraulic actuator for real-time hybrid simulation," in Mechanical Systems and Signal Processing, vol. 48, pp 260-273.

Ragonesi, D., Agrawal, S., Sample, W., and Rahman, T. (2011). "Series elastic actuator control of a powered exoskeleton," in Proc. IEEE Annual. Int. Conf. Eng. Med. Biol. Soc. pp. 3515–3518.

Robinson W., Pratt G. (2000). "Force Controllable Hydro-Elastic Actuator", Robotics and Automation, vol. 2, pp. 1321-1327.

Taylor, M. D. (2011). "A compact series elastic actuator for bipedal robots with human-like dynamic performance," Master's thesis, Robotics Inst., Carnegie Mellon Univ., Pittsburgh, PA, USA.

Tang, W., Huang, J., Wu, J., Wang, Q. (2010) "A PID tuning method based on dominant poles and phase margin," in Proceedings of the 29th Chinese Control Conference.

